

Reactive electron/molecule collisions: state-to-state cross sections and rate coefficients for modeling the kinetics of the cold plasmas

J Zs Mezei^{1,2}, E Djuiss², A Abdoulanziz², J Boffelli², F Iacob³, N Pop⁴, D Talbj⁵, V Laporta⁶,
M Ayouz⁷, V Kokouline⁸, A Bulte⁹, K Hassouni¹⁰ and I F Schneider²

¹Institute for Nuclear Research, Hungarian Academy of Sciences, H-4001 Debrecen, Hungary

²LOMC UMR CNRS 6294, Normandy University le Havre, 76058 Le Havre, France

³West University of Timisoara, 300223 Timisoara, Romania

⁴Politechnica University of Timisoara, 300223 Timisoara, Romania

⁵LUPM UMR CNRS 5299 University of Montpellier, 34095 Montpellier, France

⁶P.Las.M.I. lab, Nanotec, CNR, 70126 Bari, Italy

⁷LGPM EA CNRS 4038 CentralSupélec, University Paris Saclay, 91190 Gif-sur-Yvette, France

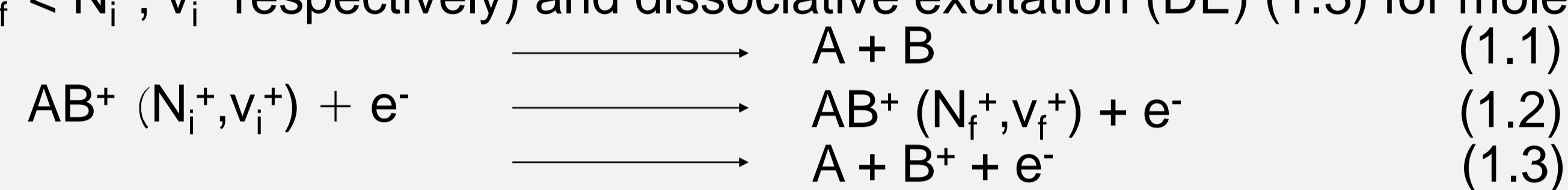
⁸University of Central Florida Orlando, 32816 Orlando, Florida, USA

⁹Complexe de Recherche Interprofessionnel en Aérothermochimie (CORIA) CNRS, Université de Rouen, France

¹⁰Laboratoire des Sciences des Procédés et des Matériaux, CNRS, Unive. Paris 13, France

Electronic collisions are major processes dominating the kinetics of cold non-thermal ionized media such as interstellar molecular clouds, polar aurorae, fusion edge plasmas, shock layers of atmospheric reentries, propulsion gases and plasmas assisting ion implantation and combustion.

Using the Multichannel Quantum Defect Theory (MQDT) [1-3], R-matrix Theory [4] and Configuration Interaction Method (boomerang model)[5], we computed cross sections and rate coefficients for the dissociative recombination (DR) (1.1) and the related competitive processes – (ro)vibrational excitation or de-excitation (RVE or RVdE) (1.2) ($N_f^+, v_f^+ > N_i^+, v_i^+$ or $N_f^+, v_f^+ < N_i^+, v_i^+$ respectively) and dissociative excitation (DE) (1.3) for molecular cations :



where $v_{i,f}^+$ and $N_{i,f}^+$ stand for the initial or final vibrational and rotational quantum number of the target ion.

The description of the quantum dynamics relies on molecular structure data previously explored. A representative sample of such data is given in Figures 1-3, taking the electron/ H_2^+ system as example.

Relevant examples are given below for various targets: AB stands for H_2^+ - Fig. 4, HD - Fig. 5, BeH - Figs. 6 and 7, BF - Fig. 8, CH - Fig. 9, CO - Fig. 10, N₂ - Figs. 11 and 12, SH - Figs. 13, 14 and 15, ArH - Fig. 16, BF₂ - Figs. 17 and 18, C₂H - Fig. 19, N₂H - Fig. 20 and CH₂NH₂ - Fig. 21.

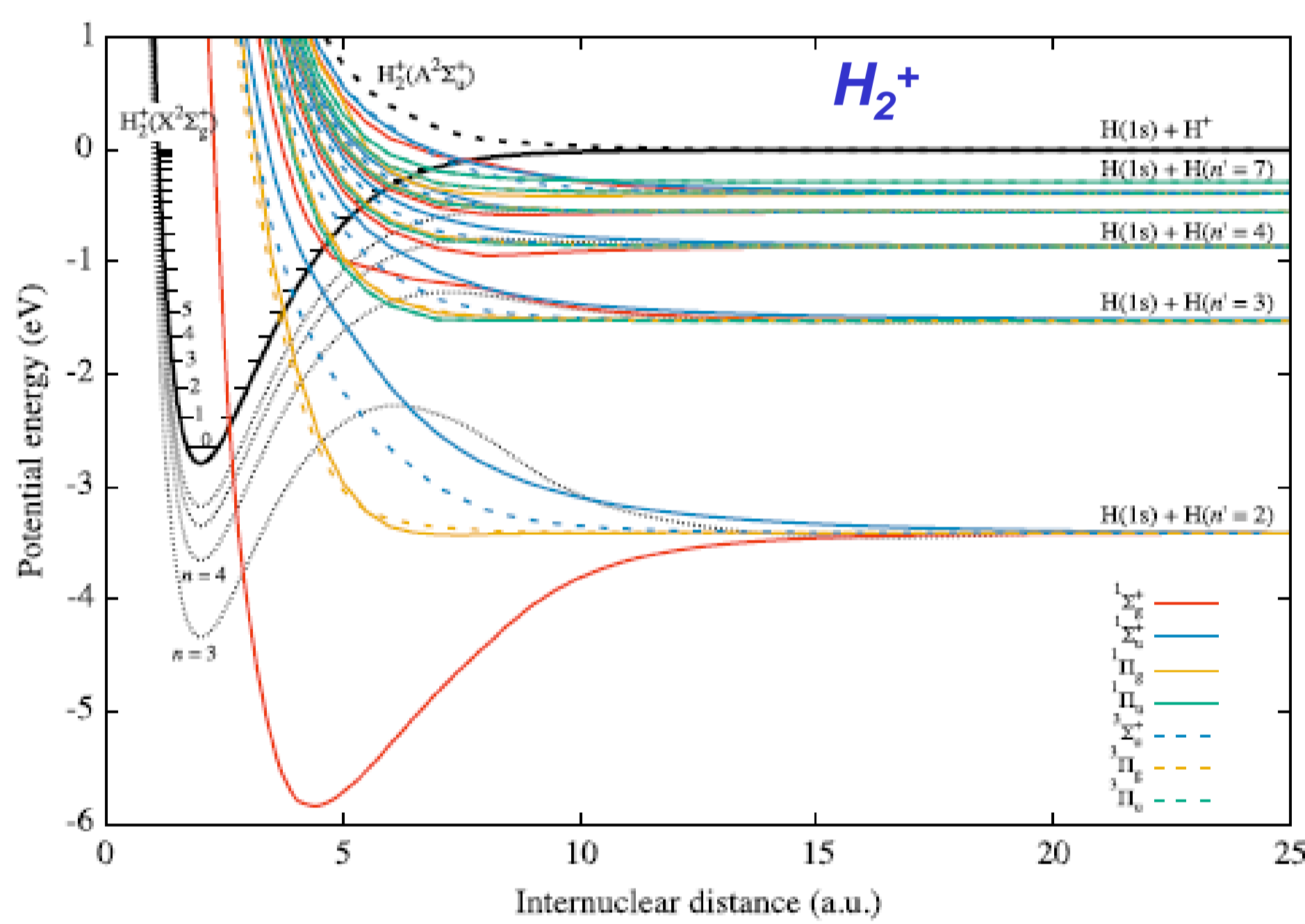


Figure 1. Summary on potential energy curves - ground rotational state - relevant for the electron/ H_2^+ reactive collisions [article in preparation].

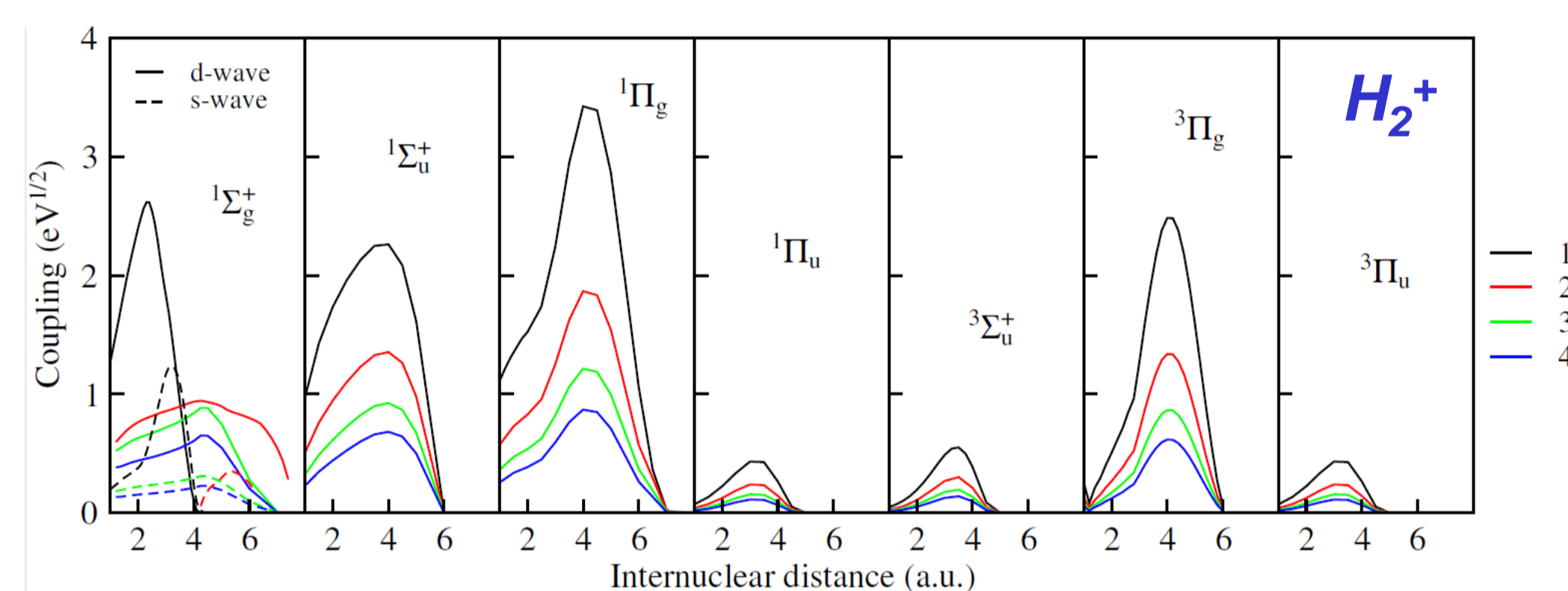


Figure 2. Discrete-to-continuum couplings for the 7 symmetries considered in the MQDT calculations. For the symmetry $1\Sigma_g^+$ both contributions coming from s- and d-partial waves are shown [article in preparation].

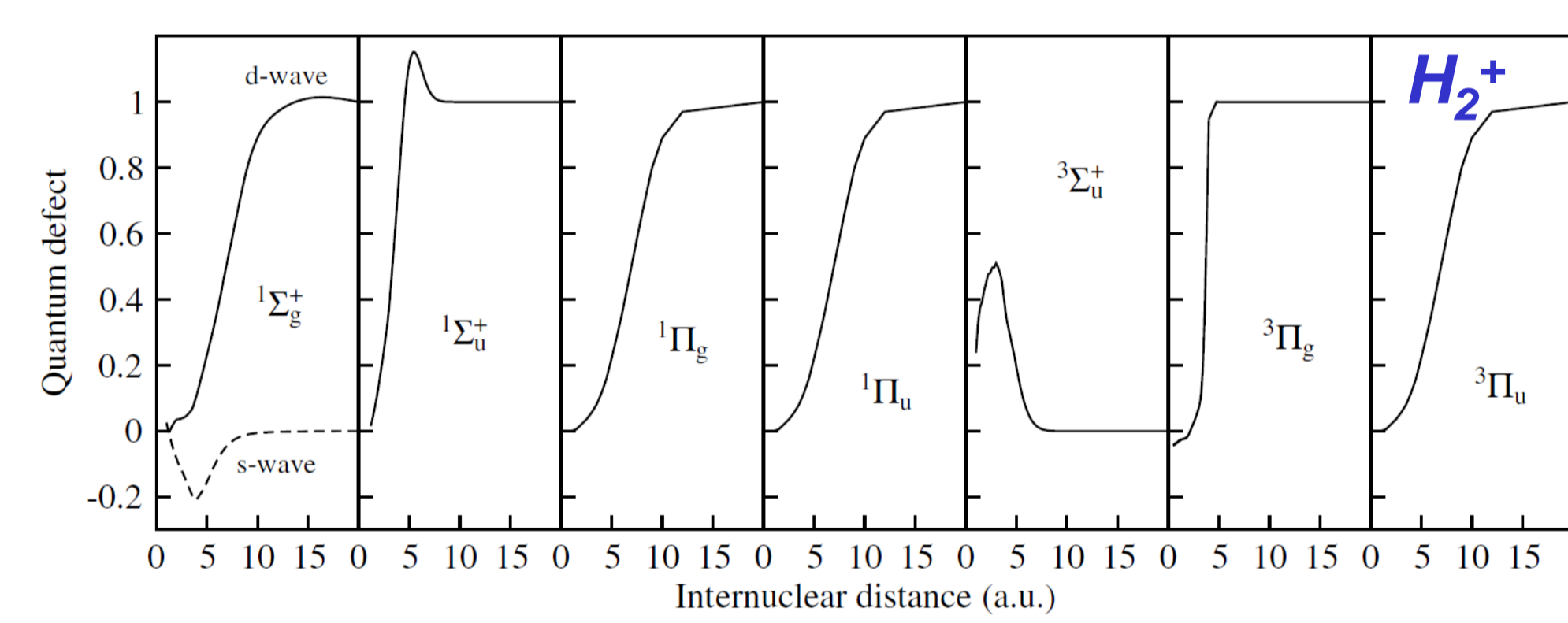


Figure 3. Rydberg states quantum defects for the 7 symmetries considered in the MQDT calculations. For the symmetry $1\Sigma_g^+$ both contributions coming from s- and d-partial waves are shown [article in preparation].

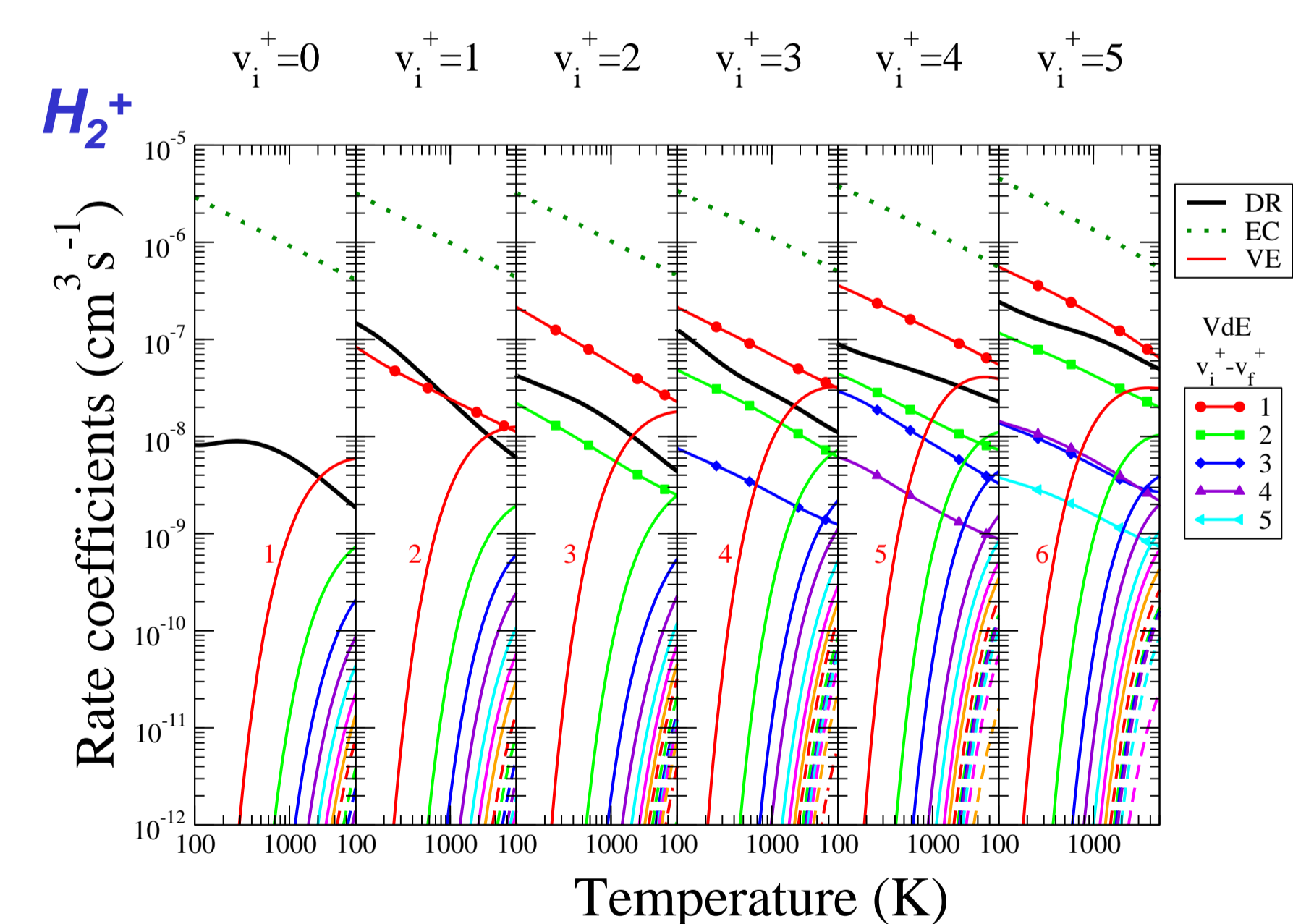


Figure 4. Maxwell isotropic rate coefficients for the DR and state-to-state VE, VdE of H_2^+ ion [article in preparation].

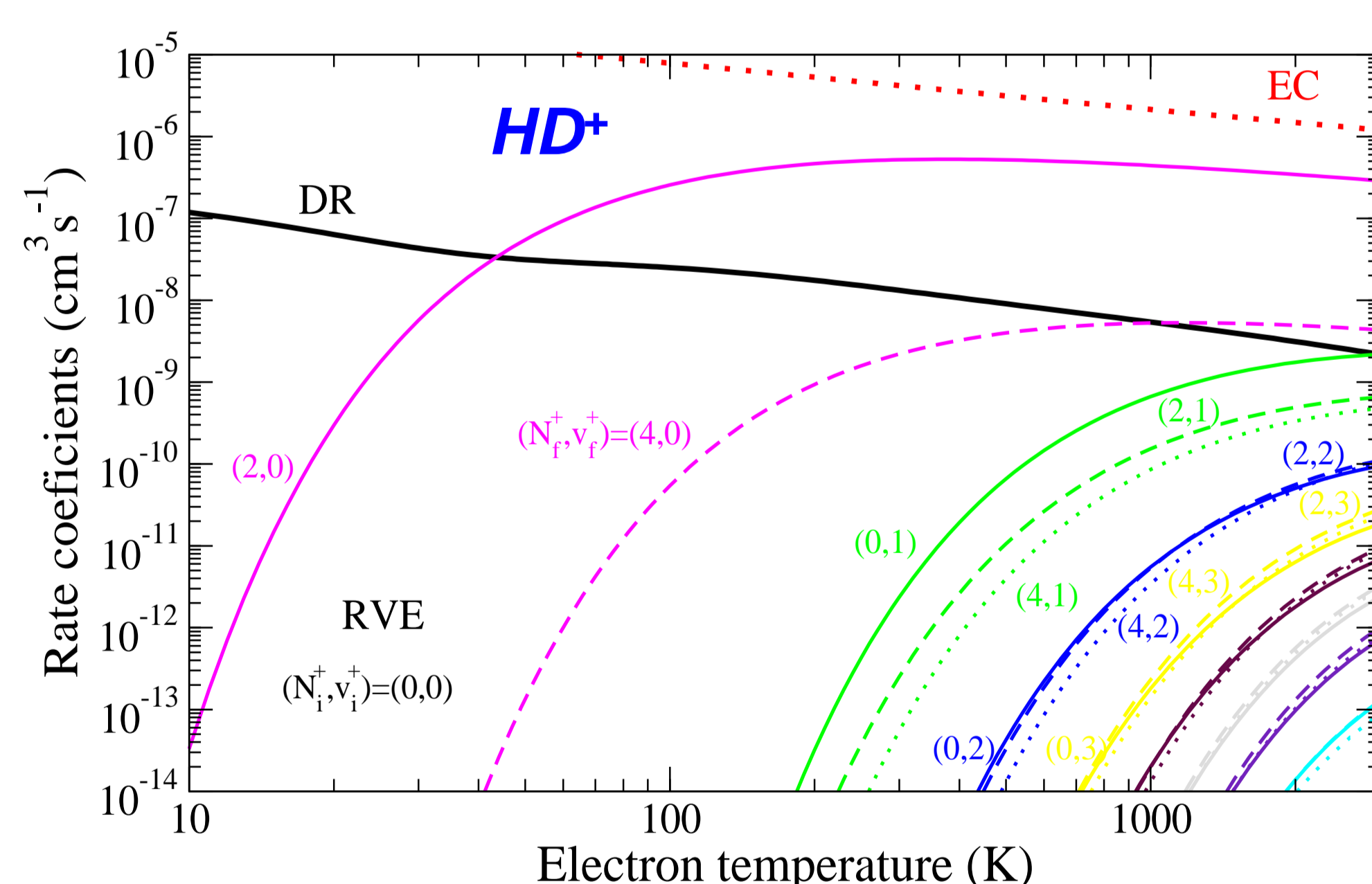


Figure 5. Rate coefficients for Dissociative Recombination (DR), Elastic Collisions (EC) and RoVibrational Excitation (RVE) of HD^+ in its ground state [6].

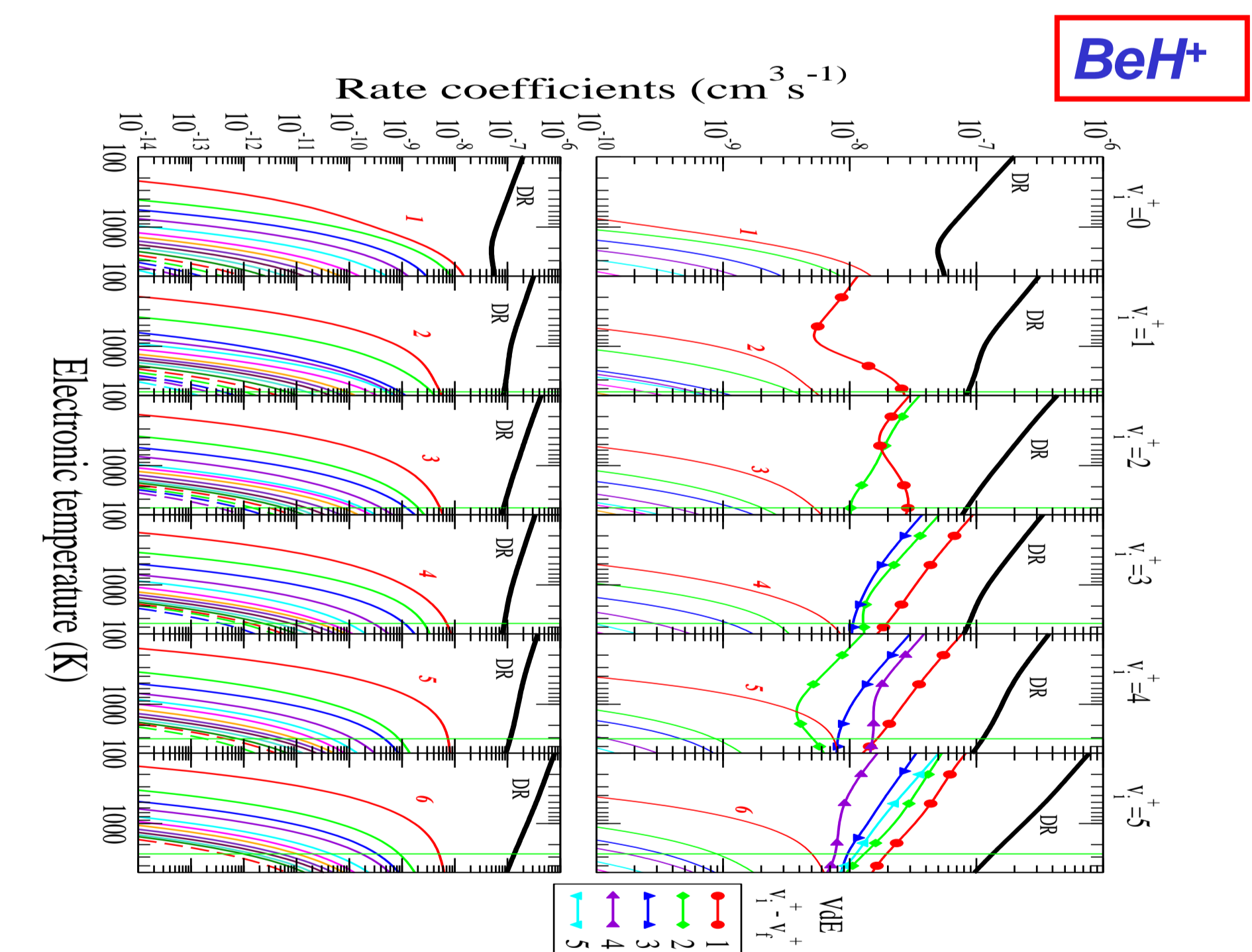


Figure 6. Maxwell rate coefficients for the DR, VE and VdE of BeH^+ ion in its electronic ground state and on its initial vibrational states v_i^+ [7]. The numbers label the final vibrational state of the transition.

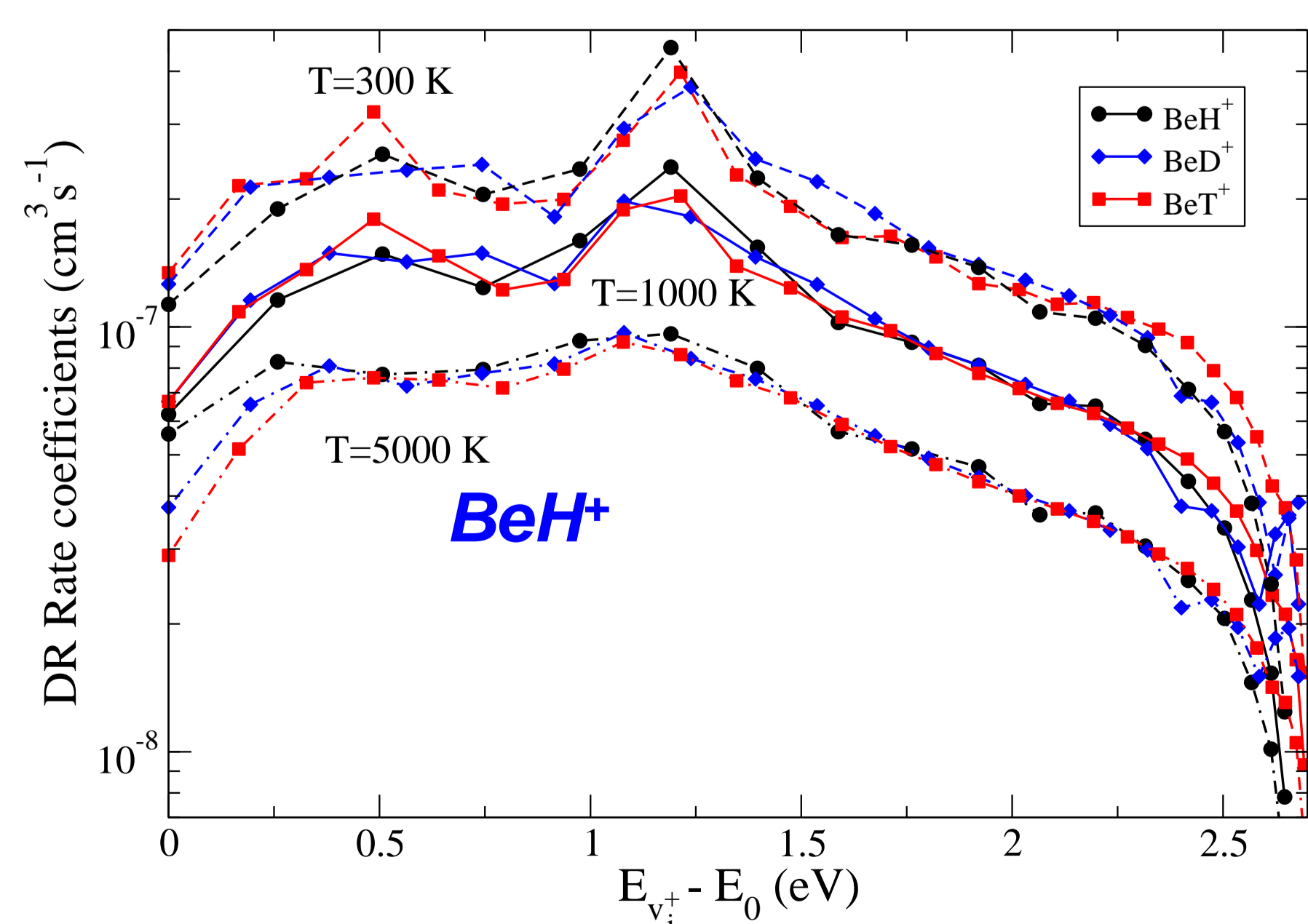


Figure 7. Rate coefficients for DR of BeH^+ [7,8,9], BeD^+ [10] and BeT^+ as a function of the vibrational energy: isotopic effects.

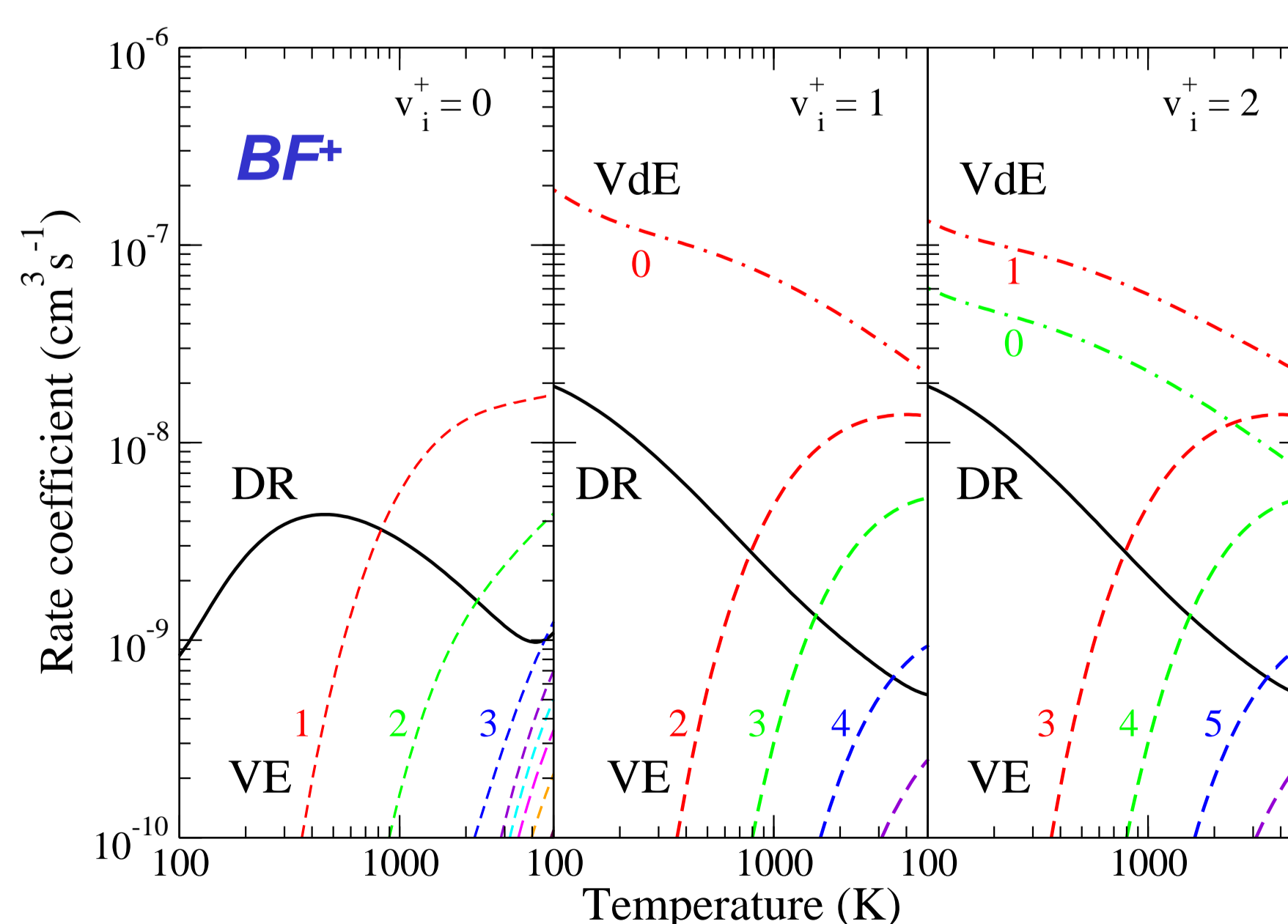


Figure 8. Maxwell rate coefficients for the DR, VE and VdE of BF^+ ion in its electronic ground state and on its initial vibrational states v_i^+ [11]. The numbers label the final vibrational state of the transition.

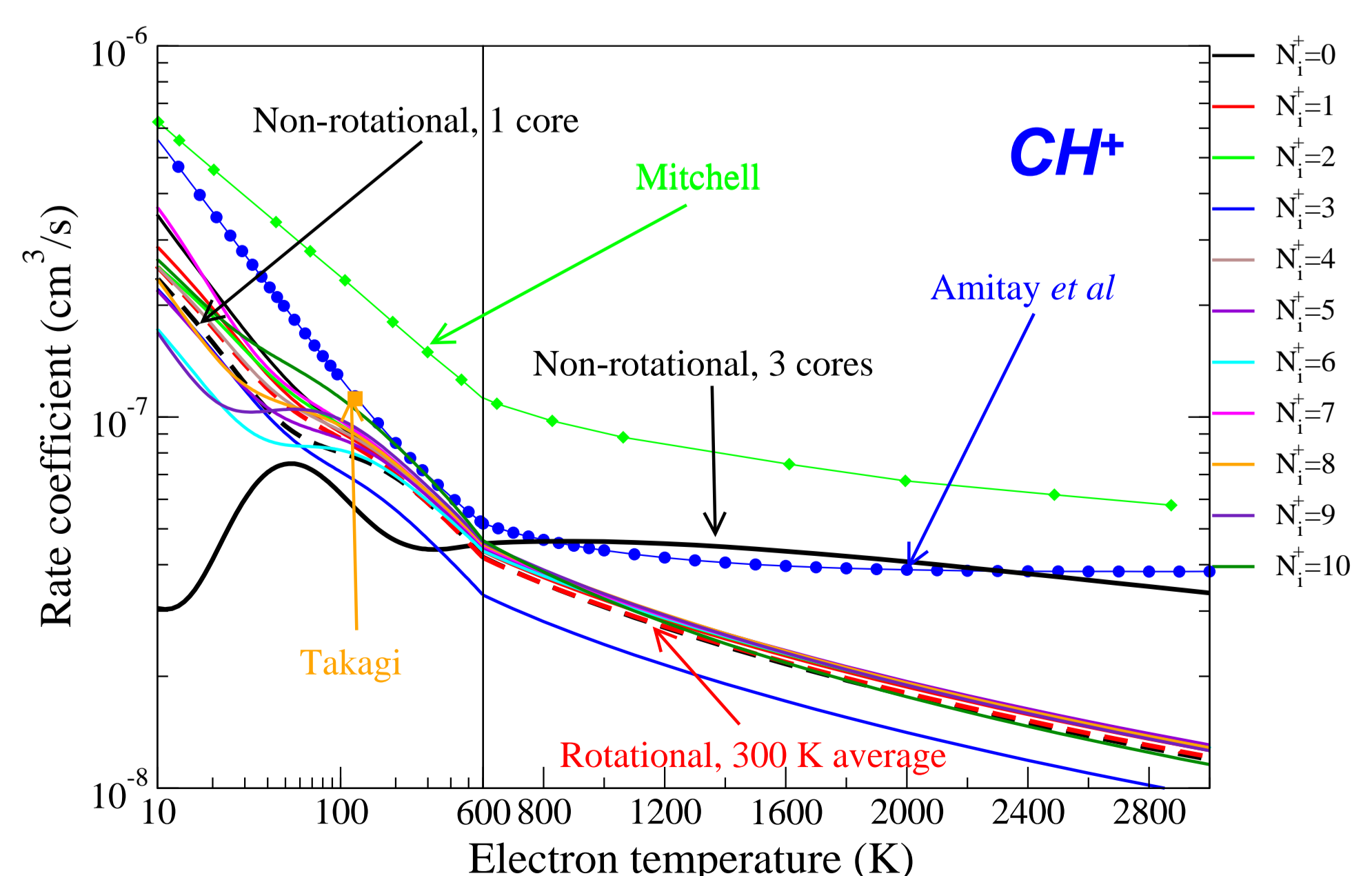


Figure 9. Dissociative Recombination rate coefficients of CH^+ : Rotational and core excited effects. Comparison with experiments [12-16] and other theoretical calculation.

(following) Reactive electron/molecule collisions: state-to-state cross sections and rate coefficients for modeling the kinetics of the cold plasmas

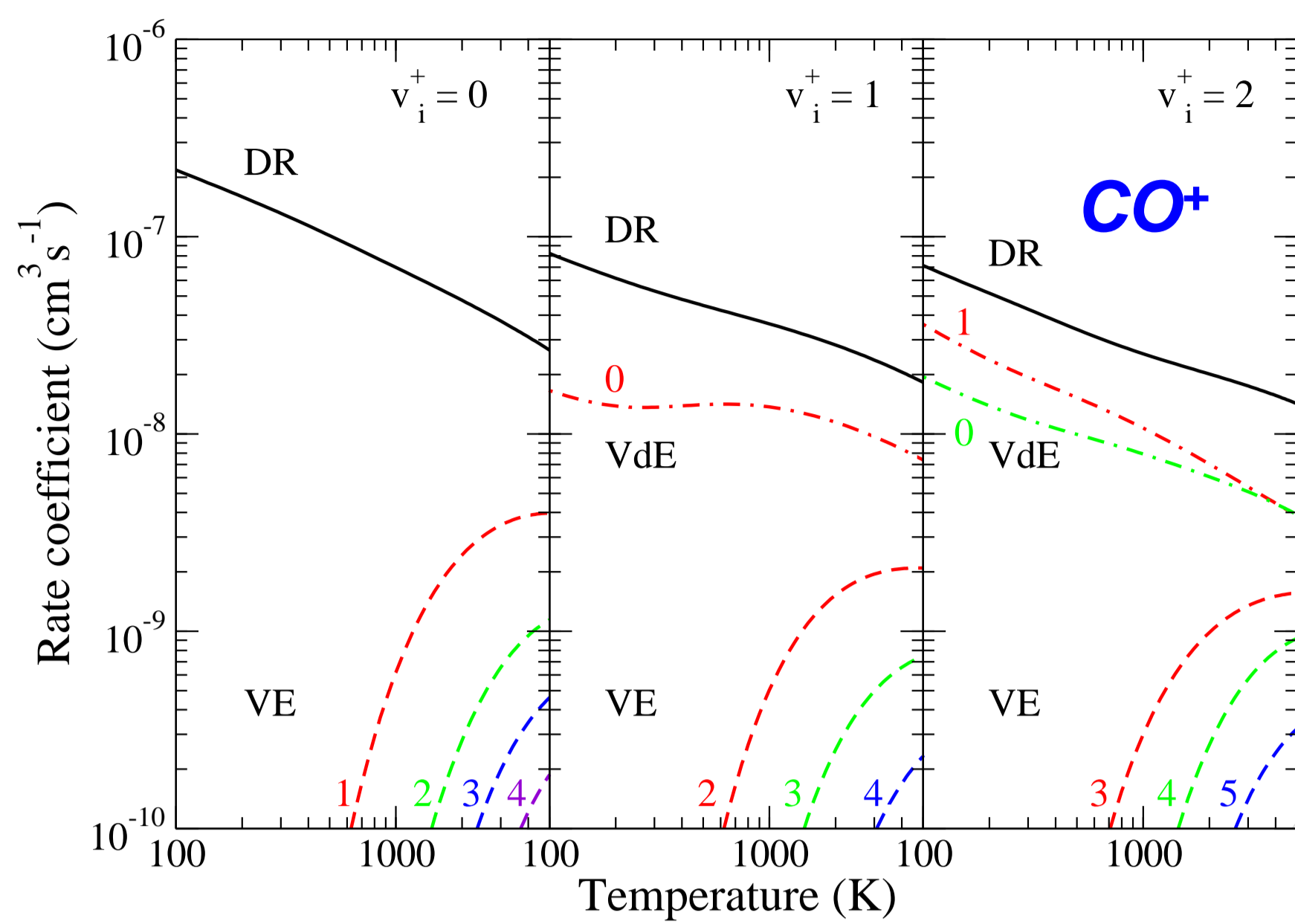


Figure 10. DR, VE and VdE rate coefficients for a vibrationally relaxed CO^+ target [17].

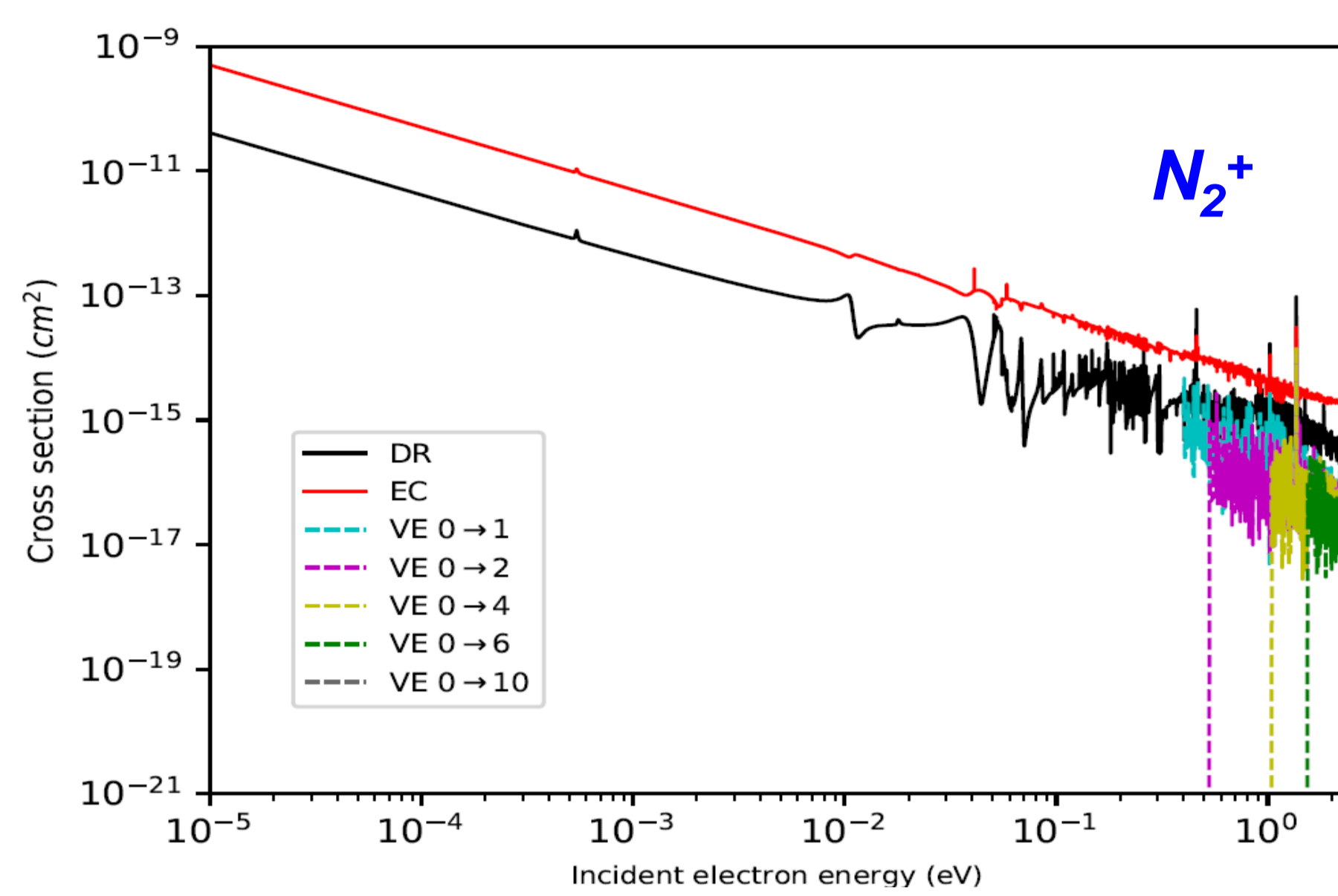


Figure 11. Dissociative Recombination (DR) and Vibrational Excitation (VE) cross section for N_2^+ in its ground state [18].

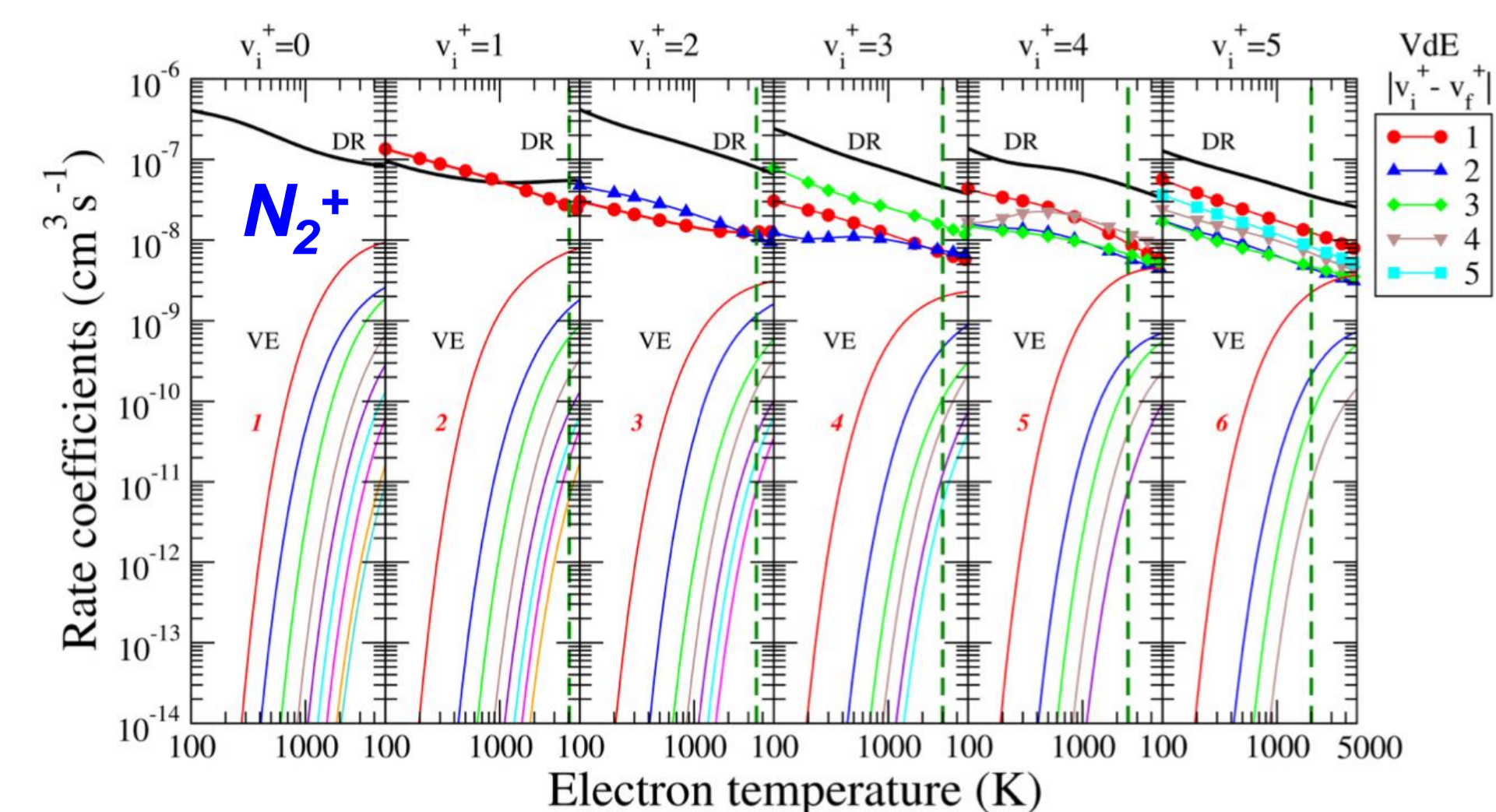


Figure 12. Dissociative Recombination (DR), Vibrational Excitation (VE) and Vibrational De-excitation cross sections for N_2^+ in its lowest 6 vibrational states [19].

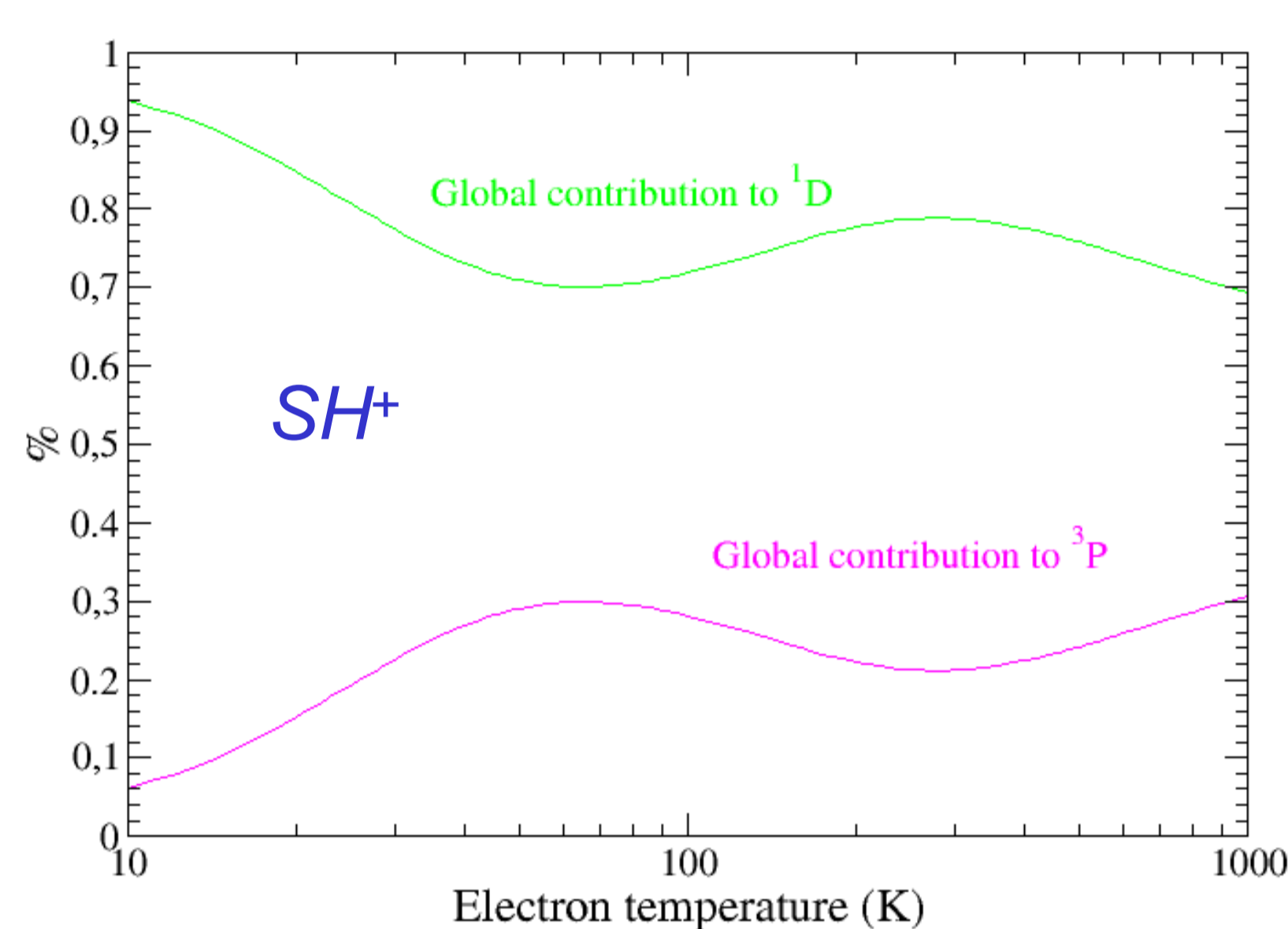


Figure 13. Yield (in percents) of the global contributions to the two sets of atomic fragments [article in preparation].

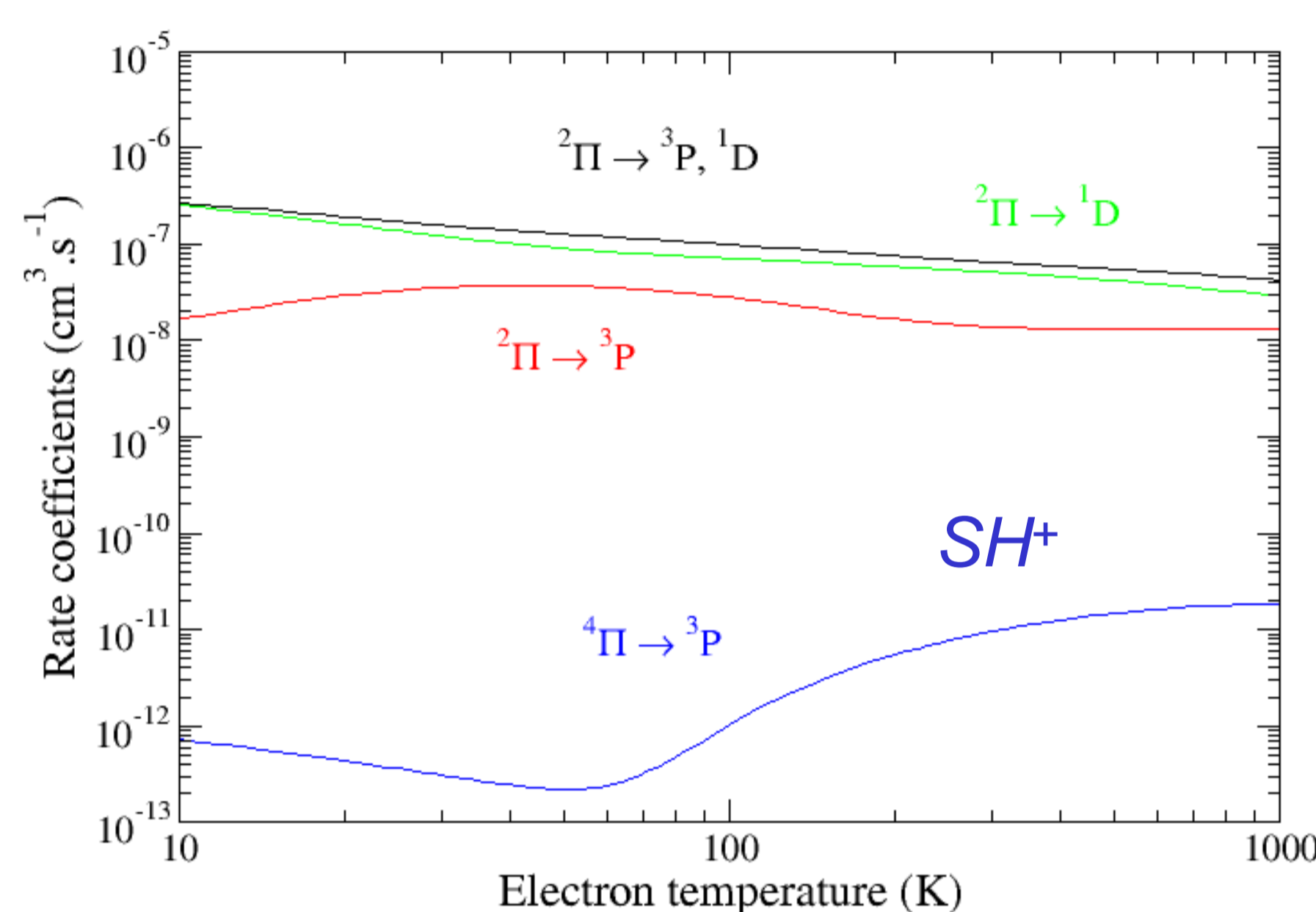


Figure 14. Partial DR's rate coefficients leading to the $\text{S}(3\text{P})+\text{H}(2\text{S})$ and $\text{S}(1\text{D})+\text{H}(2\text{S})$ atomic fragments [article in preparation].

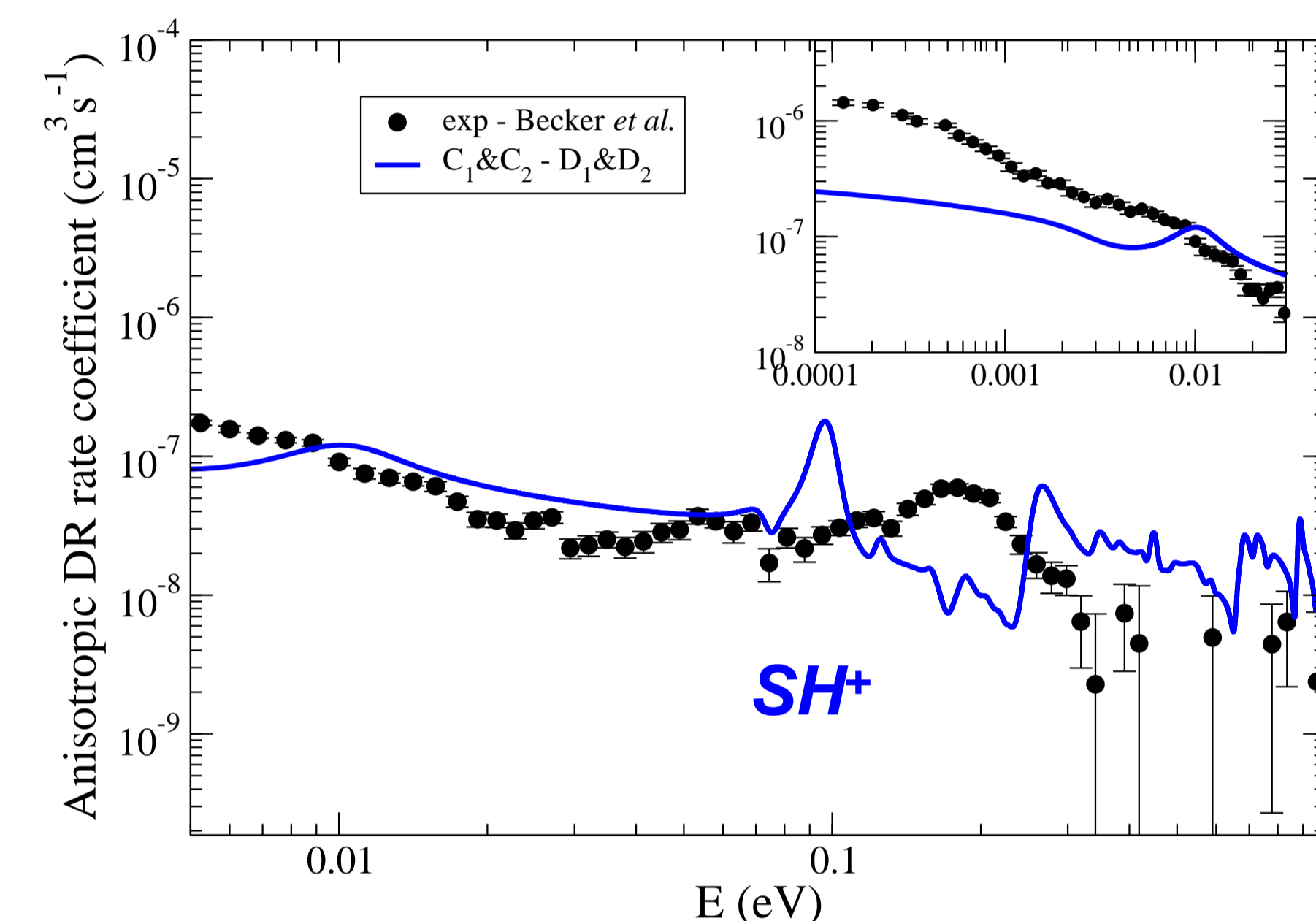


Figure 15. Anisotropic rate coefficients for DR of SH^+ [20] compared with TSR measurements [21].

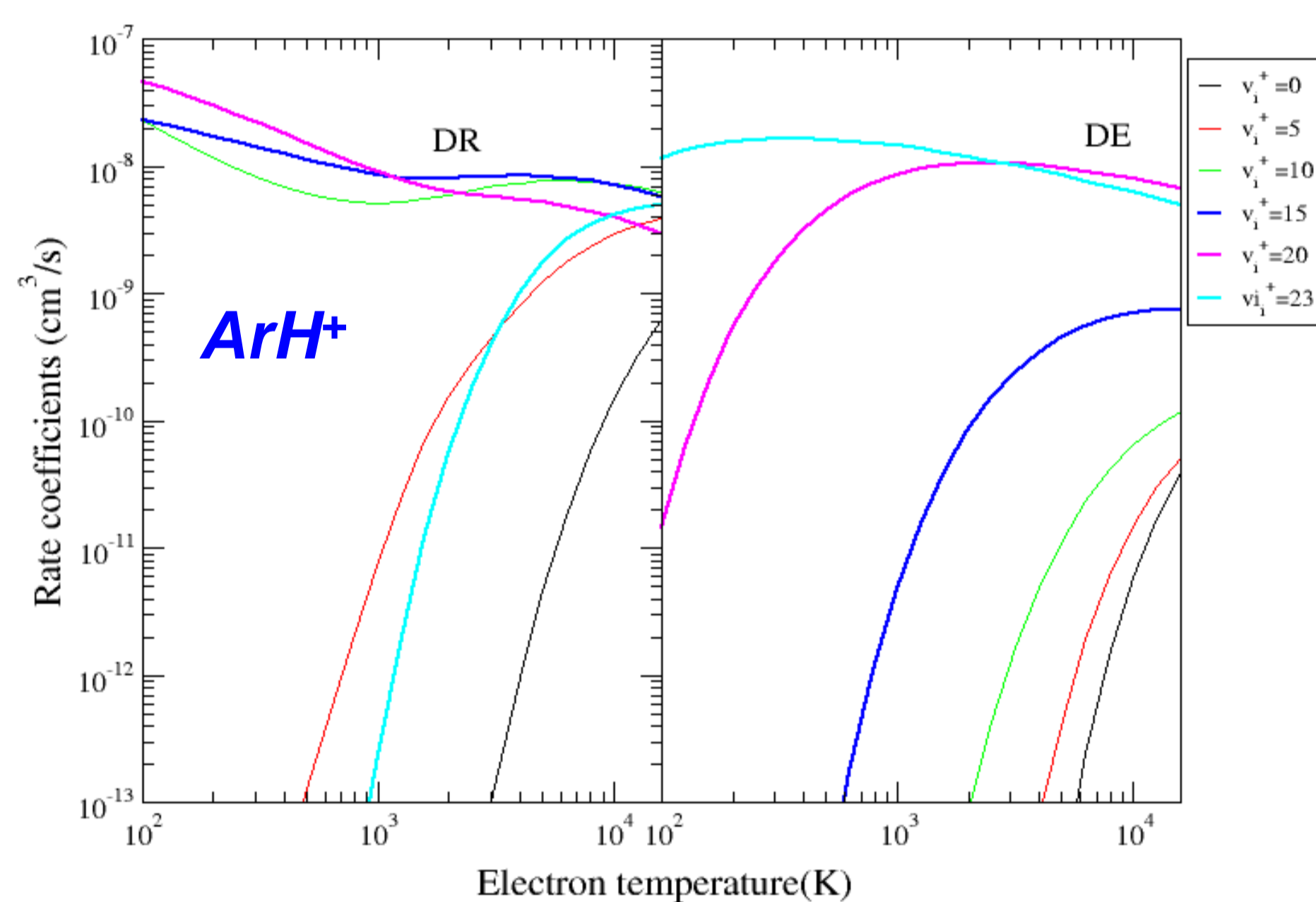


Figure 16: Rate coefficients for DR and DE. $v_i^+ = 0, 5, 10, 15, 20$ and 23 of ArH^+ [article in preparation]

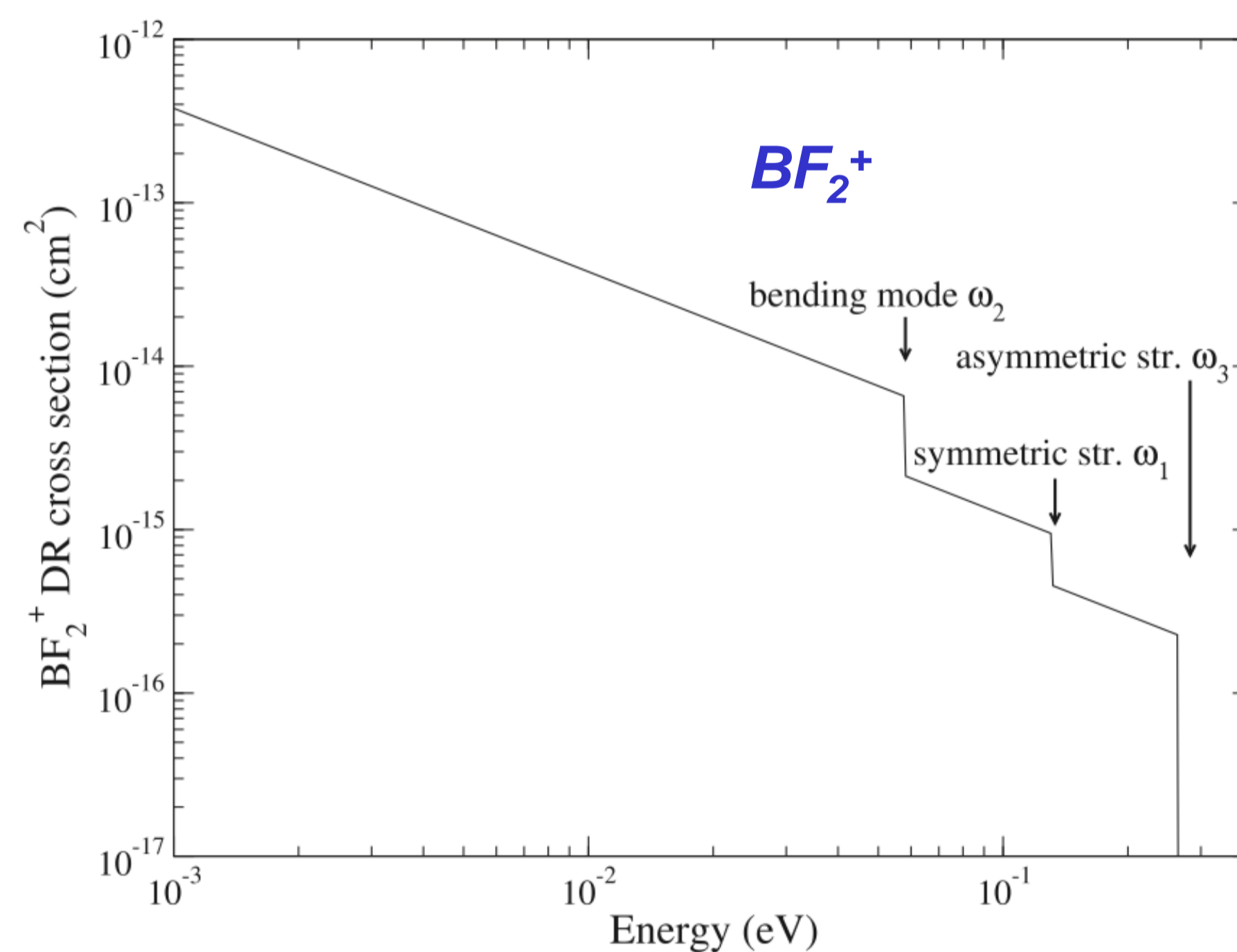


Figure 17. Cross section for Dissociative Recombination (DR) of BF_2^+ radicals [11].

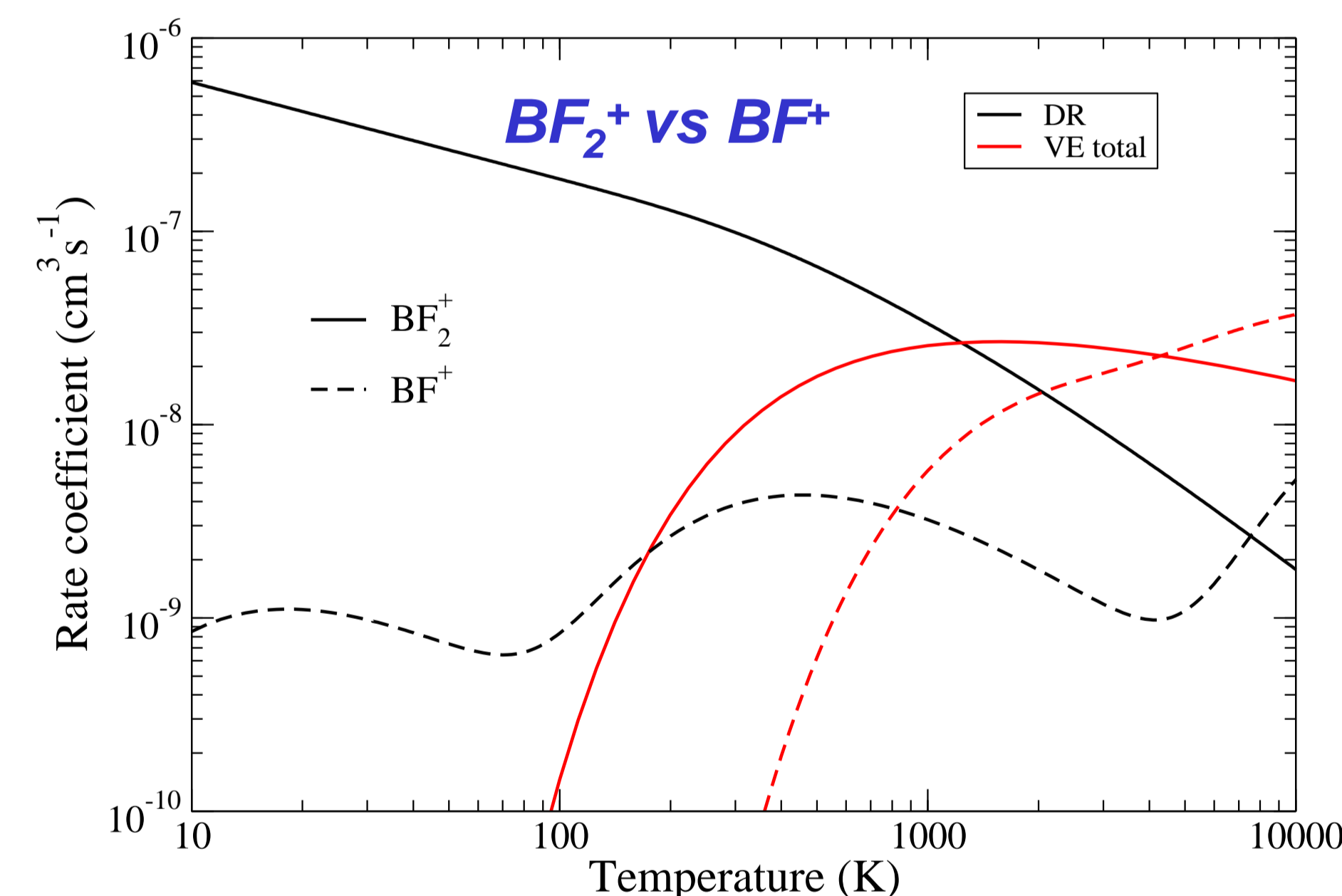


Figure 18. Rate coefficients for Dissociative Recombination (DR) and Vibrational Excitation (VE) of BF^+ [11] and BF_2^+ radicals [22].

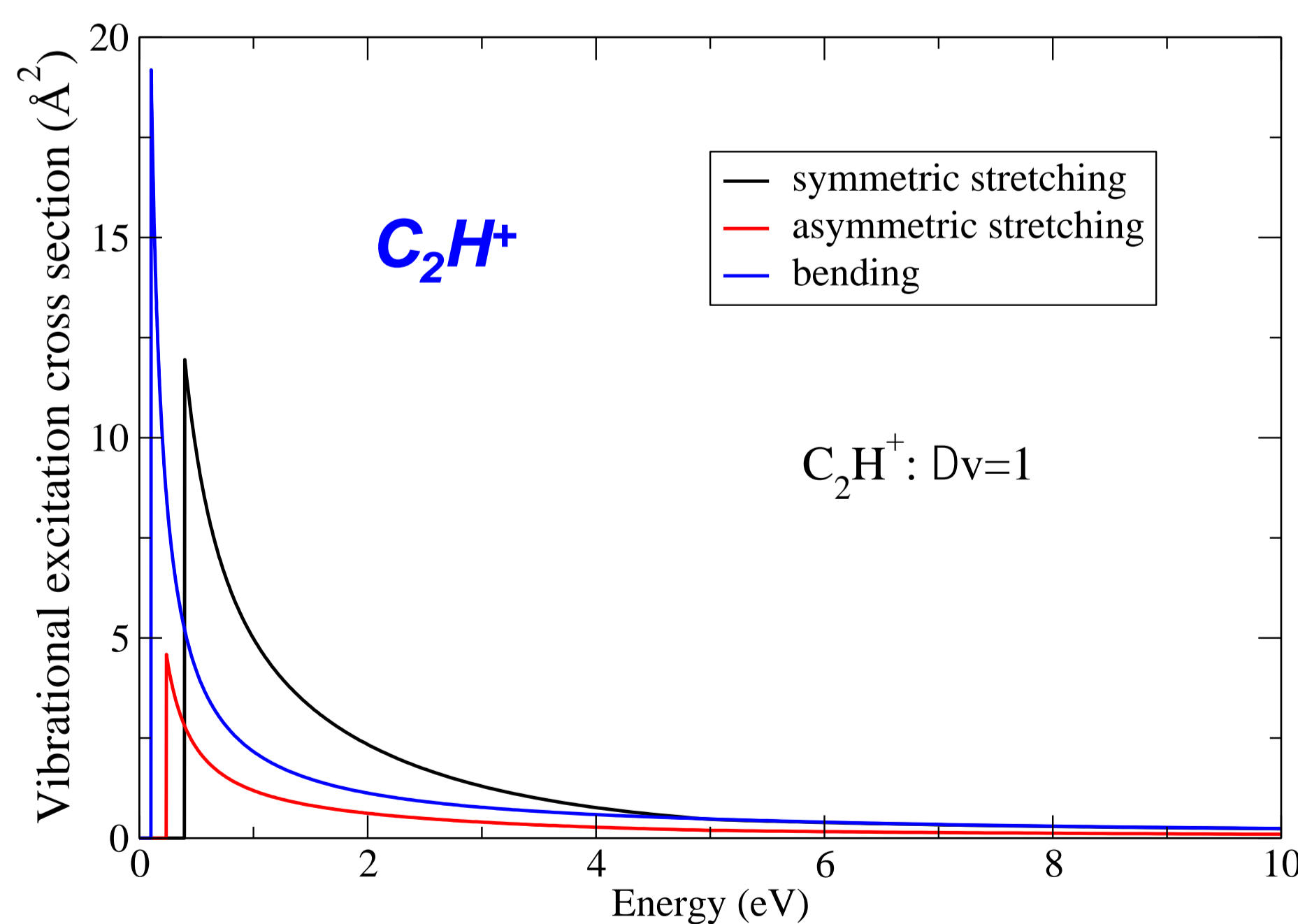


Figure 19. VE cross sections for the normal modes of C_2H^+ in its ground state [article in preparation].

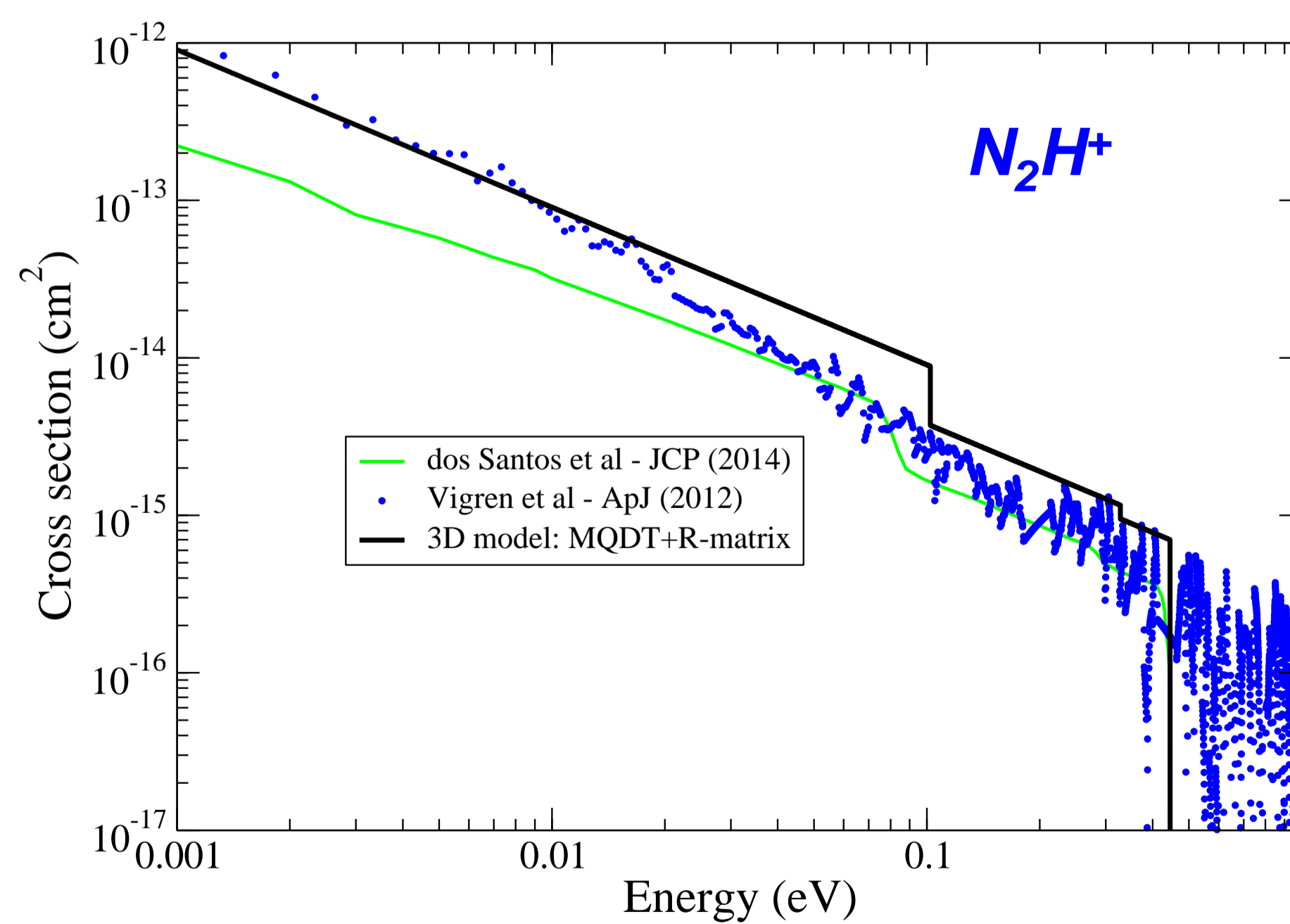


Figure 20. DR cross sections for N_2H^+ in its ground state [article in preparation].

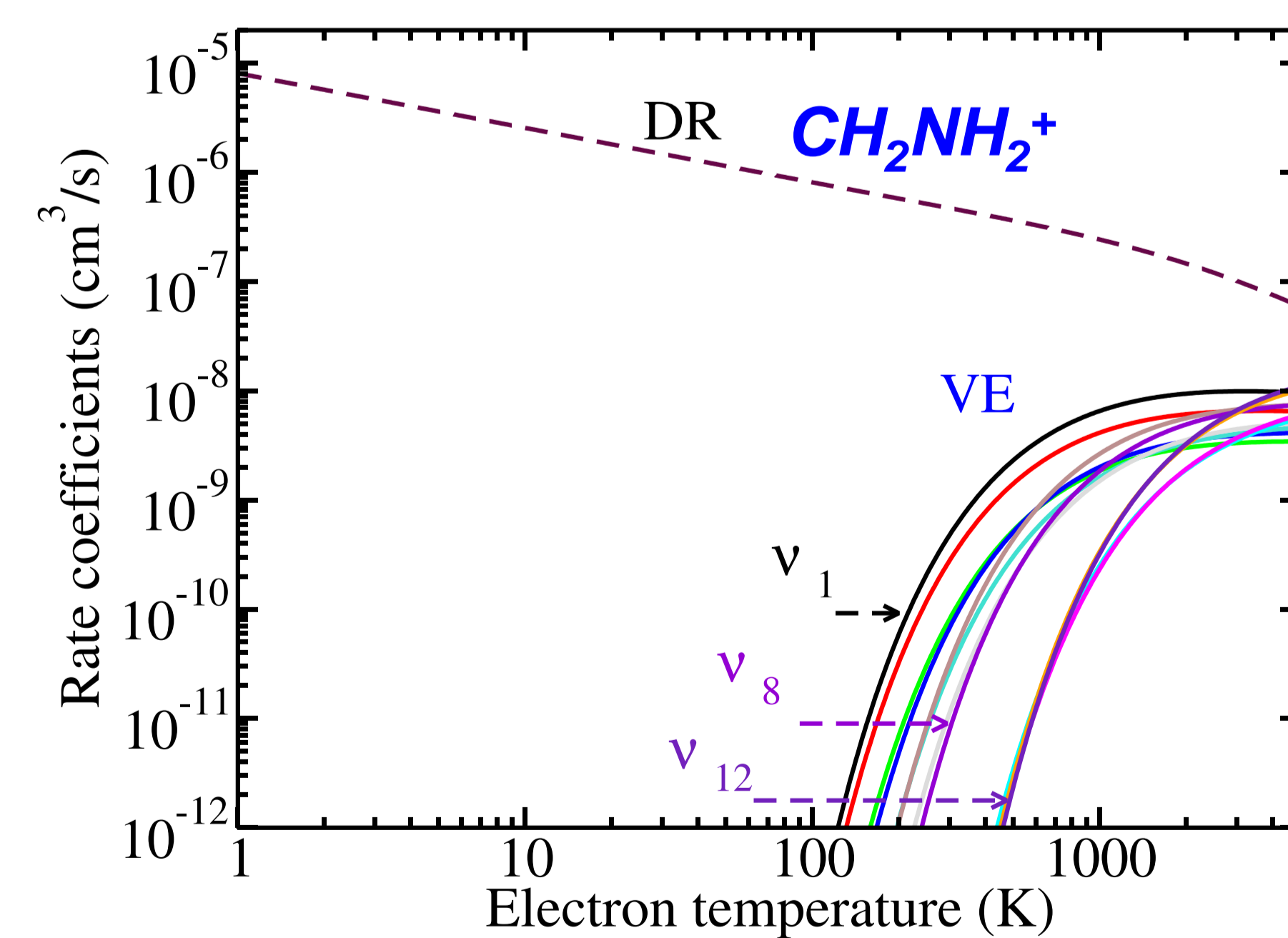


Figure 21. DR and VE rate coefficients of CH_2NH_2^+ in its ground state [23].

References

- [1] Giusti A 1980. Phys. B **13** 3867
 [2] Schneider I F et al 1991. Phys. B **24** L289
 [3] Mezei J Zs et al 2019 ACS Earth and Space Chem. **3** 2376
 [4] Tennyson J. 2010 Phys. Rep. **491** 29
 [5] Barassey N 1968. Phys. B. At. Mol. Phys. **1** 349
 [6] DULSI E, et al 2020 Romanian Astron. J., Vol. 1, No. 1
 [7] Niyonzima S et al, 2013 Phys. Rev. A **87** 022713
 [8] Laporta V et al, 2017 Plasma Phys. Control Fusion **59** 045008
 [9] Niyonzima S et al 2017 APNDT **115-116** 287
 [10] Niyonzima S et al 2018 PSSST **27** 025015
 [11] Mezei J Zs et al 2016 PSSST **25** 055022
 [12] Mezei J Zs et al 2019 ATOMS **7** 82
 [13] Chakrabarti K et al 2018. J. Phys. B **51** 104002
 [14] Amitay Z et al 1996, Phys. Rev. A **54** 4032
 [15] Mitchell J B A et al 1978 Astrophys. J. **222** L77
 [16] Takagi H et al 1991. Phys. B **24** 711
 [17] Moulane Y et al 2018 ASA **615** A53
 [18] Little D A et al 2014 Phys. Rev. A **90** 052705
 [19] Abdoulanziz A et al 2021. J. of Applied Phys. **129**, 053303
 [20] Kashinski D et al, 2017. Chem. Phys. **146** 204109
 [21] Becker A 2016, PhD thesis, Univ. Heidelberg
 [22] Kokorouline V et al, 2018 PSSST **27** 115007
 [23] Yuen C H et al 2019 MNRAS **484** 659

Acknowledgments

The authors acknowledge the Normandy region and the FEDER via the CO_2 VIRIDIS and BIOENGINE projects, ANR via the MONA and LabexEMC3/Ptolémée projects, and the IEPF research federation. The authors are grateful for the financial support from the National Research, Development and Innovation Fund of Hungary via the project FK19 132989 and NKFIH-TET and PHC Balaton projects.